

#### Central European Journal of Chemistry

# Microstructure of brushite crystals prepared via high internal phase emulsion

**Research Article** 

Hong N. Lim<sup>1\*</sup>, Anuar Kassim<sup>1</sup>, Nay M. Huang<sup>2</sup>, Chin H. Chia<sup>3</sup>

<sup>1</sup> Chemistry Department, Faculty of Science, University Putra Malaysia, 43400 UPM Serdang, Malaysia

<sup>2</sup> Solid State Physics Research Laboratory, Physics Department, Faculty of Science, University of Malaya, 50603 Kuala Lumpur, Malaysia

<sup>3</sup> School of Applied Physics, Faculty of Science & Technology, Universiti Kebangsaan Malaysia, 43600 Bangi, Malaysia

Received 25 May 2009; Accepted 3 September 2009

**Abstract:** For the first time, various microstructures of calcium phosphates were successfully synthesized using a high internal phase emulsion process. The crystals were possessed in the brushite crystalline phase. The morphology of the crystals was influenced by the variables related to the emulsion process route, which consisted of flakes, dendrites and particulates structures.

Keywords: Concentrated emulsion • Calcium phosphates • Electron microscopy

© Versita Warsaw and Springer-Verlag Berlin Heidelberg.

### 1. Introduction

Calcium orthophosphates are salts of tribasic phosphoric acid,  $H_3PO_4$ , and its ionic compounds. Hydroxyapatite (HAP)  $Ca_5(PO_4)_3(OH)$ , octacalcium phosphate (OCP)  $Ca_8H_2(PO_4)_6 \cdot 5H_2O$ , monetite  $CaHPO_4$ , and brushite  $CaHPO_4 \cdot 2H_2O$  are different crystalline orthophosphates that have been extensively studied for their relevance in biological mineralization [1]. They can be rapidly integrated into the human body as they are bioactive and constitute the major inorganic phase of human hard tissues like the bone and teeth [2,3].

As they are osteoconductive and help in growth and attachment of bone [4,5], many researchers are driven to explore the fabrication of calcium phosphate particles of various morphologies such as lath [6], rod [7], belt [8], sheet, needle [9], wire [10], and cone [11]. Among the processing routes used to fabricate the particles are sol-gel [12], solid state [13], biosynthesis [14], chemical precipitation [1], hydrothermal [15,16], hard templating [7], emulsion [17,18] and microemulsion [6]. However, these methods give rise to particles of limited porosity, which are as equally important as the dense calcium phosphates.

Porous structures of ceramics are necessary for controlled bioactivity and bioresorbability [19]. Hulbert et al. [20] demonstrated that porous discs of near inert ceramic, exhibited thinner fibrous encapsulation with faster healing to the surrounding muscle and connective tissue when compared with dense discs of the same composition implanted in the same site. It was postulated that this is the result of mechanical interlock, which reduces the motion between the host tissue and implant, eliciting a more passive response from the host [21].

One method to introduce porosity into calcium phosphates is to use high internal phase emulsions (HIPEs) as the reaction media. They are well-known for their use in the preparation of meso/macroporous materials [22,23] and have a volume a fraction of the dispersed phase (Ø) larger than the maximum packing volume fraction ( $\emptyset_{\rm max}$ ) of 0.73, therefore allowing the droplets to just touch each other [24].

In this work, different morphologies of calcium phosphates were successfully synthesized through olein oil-in-water HIPE for the first time. The continuous water phase of HIPE in a submicron size acted as a

reactor, which allowed the reaction between calcium and phosphate ions to take place. The crystallinity of the as-prepared calcium phosphates was identified using an x-ray diffractometer and their morphologies were observed using a scanning electron microscope.

# 2. Experimental procedure

In order to fabricate calcium phosphates through the HIPE processing route, two aqueous solutions containing (a) 5 wt% Brij 35 (Fluka) and 0.50 M calcium ion and (b) 5 wt% Brij 35 and 0.30 M phosphate ion were prepared. The calcium and phosphate precursors were purchased from Sigma-Aldrich and were calcium chloride (CaCl $_2$ ), calcium nitrate (CaNO $_3$ ), disodium hydrogen phosphate (Na $_2$ HPO $_4$ ) and ammonium dihydrogen phosphate (NH $_4$ H $_2$ PO $_4$ ). Refined-bleached-deodorized (RBD) palm olein (Moi Foods Malaysia Sdn. Bhd.) as oil phase was added drop wise into each of the aqueous phase equally while stirring. The oil volume fraction (Ø) was fixed at 0.80, which was calculated based on Eq. 1.

$$\emptyset = m_o/\rho_o/[(m_o/\rho_o) + (m_w/\rho_w)] \tag{1}$$

where  $m_o/\rho_o$  is the volume of oil and  $m_w/\rho_w$  is the volume of water [25].

The mixtures were then mixed at 1500 rpm using a Multimix CKL mixer at room temperature to form HIPE and were then allowed to age to permit the formation of the calcium phosphates. Mixing was carried out by stirring or homogenizing. Stirring to blend the oilwater mixture, involves using a stainless steel shaft with one end attached to a stainless steel two-blade propeller. The stirrer promotes high flow with low shear. Homogenization is accomplished by forcing the oilwater mixture through small holes for thorough blending; this induces a relatively high shear with poorer flow characteristics. Both the methods were able to produce

homogenous HIPE. In order to retrieve the precipitates, ethanol was added to demulsify the HIPE system. The demulsified HIPE was centrifuged at 4500 rpm for 30 minutes to separate the precipitates from the HIPE system. The washing process was repeated three times with ethanol followed by deionized water. The precipitates were then calcined at 600°C for two hours to obtain powders. Bulk calcium phosphate was prepared using conventional wet chemical processing route whereby 0.50 M CaCl<sub>2</sub> aqueous solution was titrated with 0.30 M Na<sub>2</sub>HPO<sub>4</sub> aqueous solution with constant stirring as a comparison to the HIPE-prepared calcium phosphates. The variables to prepare calcium phosphates using HIPE as a reaction medium are shown in Table 1.

The crystallinity of the calcium phosphates were measured using a Phillips X-Ray Diffractometry (XRD). A thin layer of the as-prepared powder was placed on a glass slide. Measurements were taken from 4° to 70° on the 2θ scale at a size step of 0.033° s<sup>-1</sup>. The XRD data was processed using an in-built PANalytical X'pert HighScore software to examine the peak position and its corresponding intensity data. The morphology of the calcium phosphates were observed using a LEO 1455 Variable Pressure Scanning Electron Microscopy (VPSEM). The powders were mounted on aluminum stubs using double-sided tape and vacuum coated with gold in a Polaron SC500 sputter coater. The microstructure of the emulsions without the presence of calcium phosphates were examined using a Nikon optical microscope (Japan) equipped with an Infinity 2-1 digital camera (Luminera Corp., Canada) at room temperature. A small drop of the emulsion was placed onto a slide and enclosed with a cover slip. Photomicrographs were taken after equilibration for 1 minute.

Table 1. Various parameters to fabricate calcium phosphates via the HIPE processing route.

Sample	Mixing method	Mixing time	Storage temperature	Calcium source	Phosphate source
		(minute)	(°C)	(0.50 M)	(0.30 M)
BR1	Stirring	15	40	CaCl <sub>2</sub>	Na <sub>2</sub> HPO <sub>4</sub>
BR2	Homogenizing	15	40	CaCl <sub>2</sub>	Na <sub>2</sub> HPO <sub>4</sub>
BR3	Homogenizing	30	25	CaCl <sub>2</sub>	Na <sub>2</sub> HPO <sub>4</sub>
BR4	Homogenizing	30	40	CaCl <sub>2</sub>	Na <sub>2</sub> HPO <sub>4</sub>
BR5	Homogenizing	15	40	Ca(NO <sub>3</sub> ) <sub>2</sub>	NH <sub>4</sub> H <sub>2</sub> PO <sub>4</sub>

## 3. Results and Discussion

Fig. 1 shows the XRD patterns of the powders indexed to the brushite crystal structure (JCPDS file no. 2-0085) with the presence of calcium phosphate crystalline phase (JCPDS file no. 2-0647). No characteristic peaks other then the calcium phosphate phases and impurities were detected. The intensity of the diffraction peaks indicates that the samples were well-crystallized. It was found that the relative intensity at  $2\theta = 49.4^{\circ}$  for the HIPE-prepared brushite crystal is higher than the standard because of their preferential growth along a certain crystal plane due to the constraint found in the continuous phase of HIPE [26]. The result is consistent with the SEM images, and shows an elongation at a certain axis.

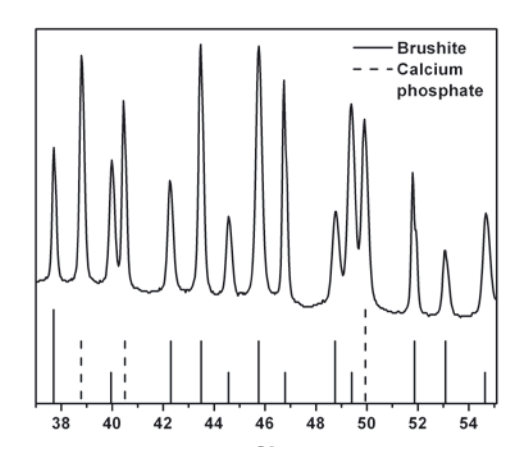


Figure 1. XRD patterns of brushite crystals

Brushite crystals prepared by the conventional processing route were bulky in size due to the absence of a templating system during preparation, as shown in Fig. 2. In contrast, the crystals obtained through the HIPE approach have smaller dimensions and unique morphologies as exhibited in the SEM images. The differences are a result of the reaction media employed, and is indicated by the emulsion. The emulsions show a template effect on the crystal growth to some extent [18]. Due to the high oil volume fraction in the HIPE system, the oil droplets come into contact and their interfaces are deformed. The deformation, caused by osmotic pressure, creates a planar film of continuous aqueous phase [37] as shown in Fig. 3. The nucleation and crystal growth take place within the geometry of the planar film. Upon aging, the resulting system is a HIPE whose continuous phase is made of solid brushite crystals. When the oil is removed from the system, the

resulting materials exhibit interesting morphologies as a result of the variables that control the HIPE processing route.

Fig. 4 shows that the morphology of brushite crystals is sensitive to the mixing method. BR1 (Fig. 4a) contains poorly defined flakes, which could be attributed to a wider continuous planar film as a result of stirring. The weak shear force induced by stirring was unable to produce a narrow droplet size distribution, which leads to droplets with high polydispersity and subsequent broader planar film. In contrast, BR2 (Fig. 4b) was prepared from homogenization and has a better defined morphology with flakes that appear to grow radially from the centre, giving rise to a flower-like appearance. This is due to a stronger shear force of homogenization and is able to produce a homogenous droplet size, which consequently gives rise to ordered planar film.

The mixing time is expected to affect the morphology of the brushite crystals. BR3 (Fig. 5a) and BR4 (Fig. 5b) have dendritic morphology because of longer period of homogenization which results in finer oil droplets and narrower planar film. BR3 represents a large quantity of sea urchin-like brushite crystals with considerable uniformity. The homogenous dendrites of BR3 are clearly shown in the inset and could be attributed to a slower nucleation and crystal growth at a lower temperature. On the other hand, high temperatures speed up the rate of collisions between the reactants and causes faster, but result in the irregular dendritic formation of BR4. These marked differences between BR3 and BR4, signifies the importance of temperature in terms of regulating the reaction to obtain a better defined morphology.

Brushite crystal formation is also influenced by the precursor type. Both BR2 and BR5 (Fig. 6) display distinctive flakes and particulate structures. The particulates of BR5 are nanosize with a narrow size distribution. This indicates that the types of precursor ions influence the lattice of calcium phosphates, which affect the stoichiometry and eventual morphology of the prepared calcium phosphates [38].

#### 4. Conclusion

Brushite crystals with various morphologies had been successfully synthesized using the HIPE processing route. The mixing method, mixing time, reaction temperature and precursor type influenced the morphology of the crystals. These variables can be carefully tuned to obtain the desired morphology of the brushite crystals to serve the many biomedical applications.

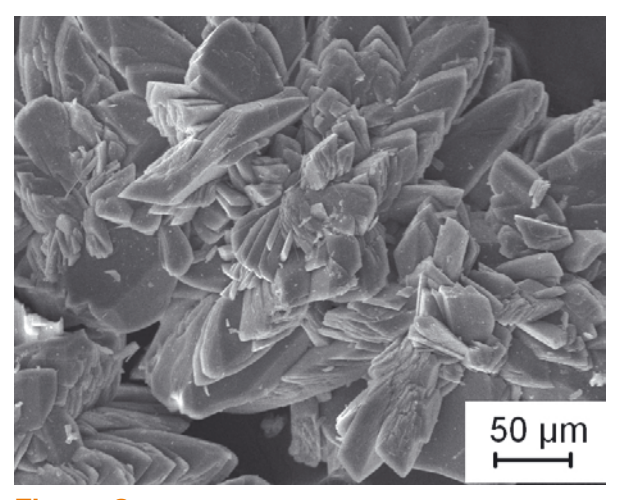


Figure 2. SEM micrograph of bulk brushite crystals

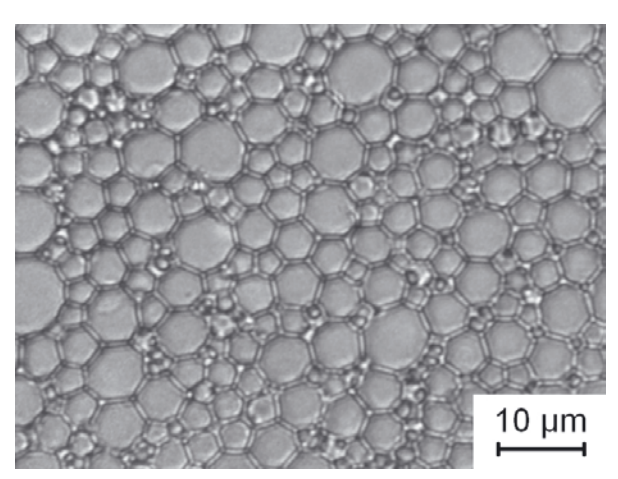


Figure 3. Microstructure of HIPE

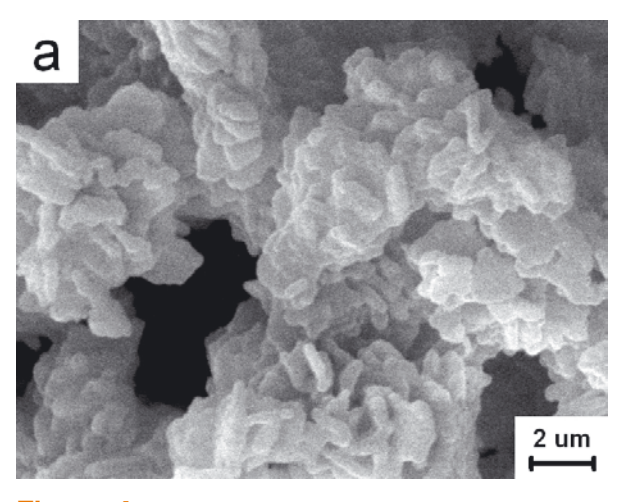
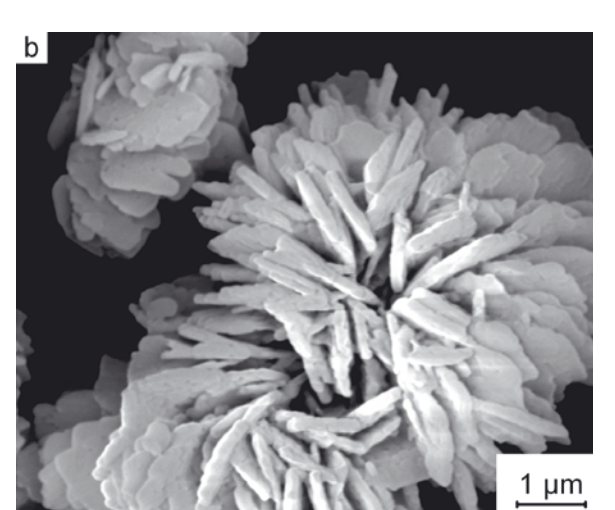


Figure 4. SEM micrographs of (a) BR1 and (b) BR2



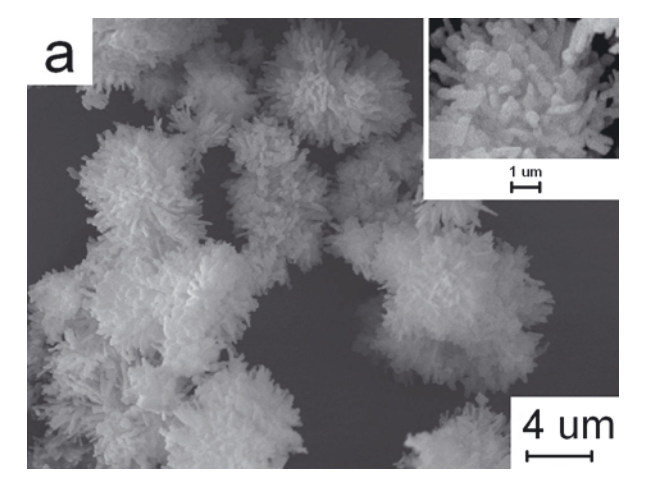
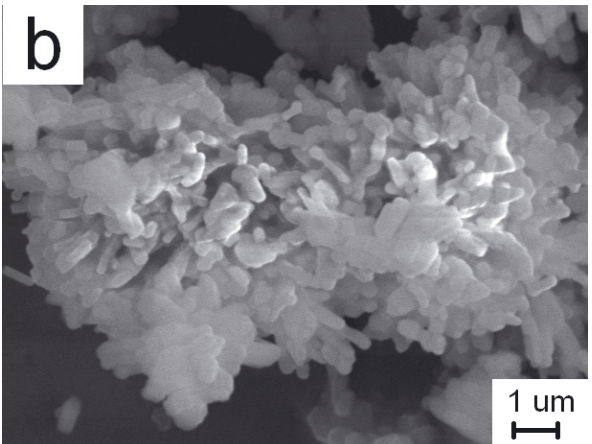


Figure 5. SEM micrographs of (a) BR3 and (b) BR4



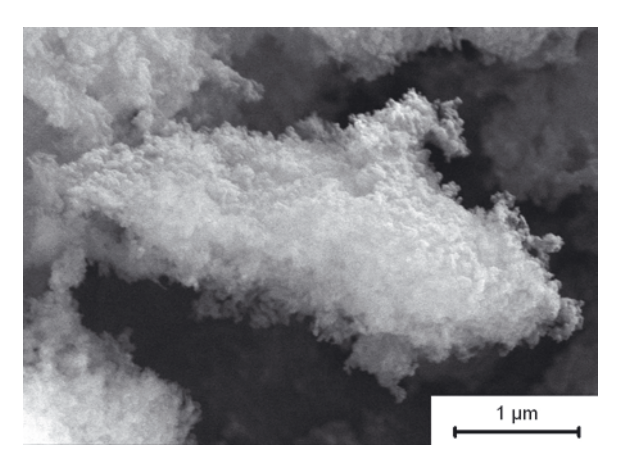


Figure 6. SEM micrograph of BR5

# **Acknowledgement**

The author (H. N. Lim) would like to thank Universiti Putra Malaysia for the Graduate Research Fellowship award.

#### References

- [1] S.M. Arifuzzaman, S. Rohani, J. Crystal Growth 267, 624 (2004)
- [2] L.L. Hench, J. Am. Ceram. Soc. 74, 1487 (1991)
- [3] S. Weiner, H.D. Wagner, Annu. Rev. Mater. Sci. 28, 271 (1998)
- [4] M. Jarcho, Clin. Orthop. Rel. Res. 157, 259 (1981)
- [5] M. Jarcho, J.F. Kay, K.I. Gumaer, R.H. Doremus, H.P. Drobeck, J. Bioeng. 1, 79 (1977)
- [6] S. Singh, P. Bhardwaj, V. Singh, S. Aggarwal, U.K. Mandal, J. Colloid Inter. Sci. 319, 322 (2008)
- [7] J. Fan, J. Lei, C. Yu, B. Tu, D. Zhao, Mater. Chem. Phys. 103, 489 (2007)
- [8] Y.J. Wang, C. Lai, K. Wei, S.Q. Tang, Mater. Lett. 59, 1098 (2005)
- [9] X.D. Kong, X.D. Sun, J.B. Lu, F.Z. Cui, Curr. Appl. Phys. 5, 519 (2005)
- [10] Y.J. Zhan, C.L. Zheng, Y.K. Liu, G.H. Wang, Mater. Lett. 57, 3265 (2003)
- [11] J.D. Hopwood, S. Mann, Chem. Mater. 9, 1819 (1997)
- [12] X. Dai, S. Shivkumar, Mater. Sci. Eng. C 28, 336 (2008)
- [13] C.S. Liu, W. Gai, S.H. Pan, Z.S. Liu, Biomaterials 24, 2995 (2003)
- [14] K.L. Yadav, P.W. Brown, J. Biomed. Mater. Res. A 65A, 158 (2003)
- [15] Y. Wang, S. Zhang, K. Wei, N. Zhao, J. Chen, X. Wang, Mater. Lett. 60, 1484 (2006)
- [16] Y. Xu, D. Wang, L. Yang, H. Tang, Mater. Charact. 47, 83 (2001)
- [17] G.K. Lim, J. Wang, S.C. Ng, C.H. Chew, L.M. Gan, Biomaterials 18, 1433 (1997)
- [18] K. Sonoda, T. Furuzono, D. Walsh, K. Sato, J. Tanaka, Solid State Ionics 151, 321 (2002)
- [19] H. Yuan, Z. Yang, J.D. de Bruijin, K. de Groot, X. Zhang, Biomaterials 22, 2617 (2001)

- [20] S.F. Hulbert, J.S. Morrison, J.J. Klawitter, J. Biomed. Mater. Res. A 6, 347 (1972)
- [21] K.A. Hing, S.M. Best, W. Bonfield, J. Mater. Sci. Mater. Med. 10, 135 (1999)
- [22] J. Esquena, G.S.R.R.R. Sankar, C. Solans, Langmuir 19, 2983 (2003)
- [23] C. Solans, J. Esquena, N. Azemar, Curr. Opin. Colloid Interface Sci. 8, 156 (2003)
- [24] R. Pal, Food Hydrocolloids 20, 997 (2006)
- [25] B. Niraula, C.K. Tan, K.C. Tham, M. Misran, Colloids Surf. A 251, 117 (2004)
- [26] N. M. Huang, et al., Mater. Lett. 63, 500 (2009)
- [27] R. Boistelle, I. Lopez-Velero, J. Crystal Growth 102, 609 (1990)
- [28] A. Ferreira, C. Oliveira, F. Rocha, J. Crystal Growth 252, 599 (2003)
- [29] P.N. Kumta, C. Sfeir, D.H. Lee, D. Olton, D.W. Choi, Acta Biomaterialia 1, 65 (2005)
- [30] M. Bohner, Injury 31, 37 (2000)
- [31] J. Lu, et al., J. Biomed. Mater. Res. 63, 408 (2002)
- [32] F. Theiss, et al., Biomaterials 26, 4383 (2005)
- [33] W. Wu, G.H. Nancollas, Pure Appl. Chem. 70, 1867 (1998)
- [34] P. Fraysinnet, L. Gineste, P. Conte, J. Fages, N. Rouquet, Biomaterials 19, 971 (1998)
- [35] L.M. Grover, J.C. Knowles, G.J.P. Fleming, J.E. Barralet, Biomaterials 24, 4133 (2003)
- [36] G. Penel, N. Leroy, P. Van Landuyt, B. Flautre, P. Hardouin, J. Lemaitre, G. Leroy, Bone 25, 81 (1999)
- [37] M.D. Lacasse, G.S. Grest, D. Levine, T.G. Mason, D.A. Weitz, Phys. Rev. Lett. 76, 3448 (1996)
- [38] M. Vallet-Regi, J. M. Gonzalez-Calbet, Prog. Solid State Chem. 32, 1 (2004)